

Sbacchiite, Ca_2AlF_7 , a new fumarolic mineral from the Vesuvius volcano, Napoli, Italy

ITALO CAMPOSTRINI, FRANCESCO DEMARTIN AND MASSIMO RUSSO

Running title: Sbacchiite, new fumarolic mineral from the Vesuvius volcano

Abstract

Introduction

Occurrence

Physical and optical properties

Chemical Analysis

X-ray crystallography and crystal structure determination

Description of the crystal structure and discussion

Acknowledgements

References

Table captions

Figure captions

27 Sbacchiite, Ca_2AlF_7 , a new fumarolic mineral from the Vesuvius volcano, Napoli, Italy

28
29 ITALO CAMPOSTRINI¹, FRANCESCO DEMARTIN^{1*} AND MASSIMO RUSSO²

30

31 ¹Università degli Studi di Milano, Dipartimento di Chimica, via Golgi 19, I-20133 Milano, Italy.

32 <http://orcid.org/0000-0003-2942-3990>,

33 ²Istituto Nazionale di Geofisica e Vulcanologia, Sezione di Napoli | Osservatorio Vesuviano, Via

34 Diocleziano, 328, I-80124 Napoli, Italy, <http://orcid.org/0000-0001-5161-5951>.

35

36 * Corresponding author: Francesco Demartin

37 Università degli Studi di Milano, Dipartimento di Chimica, via Golgi 19, I-20133 Milano, Italy.

38 <http://orcid.org/0000-0003-2942-3990>, E-mail: francesco.demartin@unimi.it

39

Abstract

The new mineral sbacchiite (IMA 2017-097), Ca_2AlF_7 , was found in a fossil fumarole (1944 eruption, $T \approx 80^\circ\text{C}$) at the rim of the crater of the Vesuvius volcano, Napoli, Italy, associated with gearsksutite, usovite, creedite and opal. It forms elongated crystals up to about $60\ \mu\text{m}$ in length. On the basis of PXRD measurements and chemical analysis, the mineral was recognized to be identical to the corresponding synthetic phase. Crystals are transparent or translucent and colorless, with vitreous lustre and white streak. The tenacity is brittle. The measured density is $3.08(2)\ \text{g/cm}^3$, the calculated density is $3.116\ \text{g/cm}^3$. The empirical formula, (based on 10 *apfu*) is $\text{Ca}_{2.02}\text{Mg}_{0.03}\text{Al}_{0.99}\text{F}_{6.97}$. Sbacchiite is orthorhombic, space group *Pnma*, with $a = 7.665(2)$, $b = 6.993(1)$, $c = 9.566(2)\ \text{\AA}$, $V = 512.2(2)\ \text{\AA}^3$ and $Z = 4$. The eight strongest X-ray powder diffraction lines are [$d_{\text{obs}}\ \text{\AA}(I)(hkl)$]: $3.840(45)(200)$, $3.563(85)(201)$, $3.499(100)(020)$, $2.899(55)(013)$, $2.750(30)(212)$, $2.281(20)(104)$, $2.255(52)(302)$ and $2.173(36)(131)$. The structure, was refined to $R = 0.0479$ for 457 reflections with $I > 2\sigma(I)$. The asymmetric unit contains an Al^{3+} and two independent Ca^{2+} cations and five fluorine anions. Al is octahedrally coordinated by six fluorine atoms; the arrangement of F around the 7-coordinated Ca(1) conforms to a distorted pentagonal bipyramid and that around Ca(2) to a very distorted polyhedron (C.N. 7+1). All the fluorine atoms have C.N. 3. The structure framework shows “isolated” $[\text{AlF}_6]$ octahedra, whereas the coordination polyhedra around Ca are linked by common edges [sequence: Ca(1)-Ca(2)-Ca(1)...] along $[010]$ and the same holds for the connection along $[001]$. Along $[100]$ however only the pentagonal bipyramids around Ca(1) are connected by bridging corners.

Key-words: sbacchiite; new mineral; fluoride; fumaroles; Vesuvius volcano.

Introduction

The Somma-Vesuvius volcanic complex is one of the most studied volcanoes in the World. This area is potentially very dangerous for the more than 800.000 inhabitants living on the slopes of the Vesuvius and for this reason detailed studies in various fields of geology and geophysics have been carried out in this region, which is subject to continuous monitoring. However little is known about the mineralogical phases that have formed or are forming in the fumaroles after the last eruption that occurred in 1944. The whole fumarolic area was studied by Parascandola (1951) between 1948 and 1960, when temperatures reached a maximum of about 800 °C in 1950, up to the 60s of the last century, when temperatures settled around the 460 °C (Parascandola, 1960, 1961). No quantitative information about the composition of the fumarolic fluxes at that time is reported, though the presence of HCl, Cl₂ and H₂S was indicated by Parascandola. On the basis of the mineralogical phases formed the presence of SO₂ and HF was nevertheless conceivable. Currently, temperatures of the fumaroles at eastern rim of the crater are between 70° and 80 °C, and their chemistry reflects the composition of the air so that, in such conditions, there is no deposition of minerals. On the contrary, the chemical composition of the fumaroles of the crater bottom is of hydrothermal type with the typical presence of H₂S (Chiodini *et al.*, 2001). We report here the description of the new mineral sbacchiite, Ca₂AlF₇, recently discovered in a fumarole at the rim of the crater, that was recognized, on the basis of XRPD measurements and chemical analysis, to be identical to the corresponding Ca₂AlF₇ synthetic phase (Domsele & Hoppe, 1980). The mineral and its name were approved by the IMA Commission on New Minerals, Nomenclature and Classification (IMA. 2017-097). Sbacchiite is pronounced “sbaki-ite” and named after Dr. Massimo Sbacchi (b. 1958, –), biologist and mineral collector, for his long-time field collaboration on fumarolic minerals and for his continuous supply of interesting material for study. A specimen of the holotype material is deposited in the Reference Collection of the Dipartimento di Chimica, Università degli Studi di Milano, catalogue number 2017-01 and a co-type specimen in the collection of the Museum of Osservatorio Vesuviano (Ercolano, Napoli), catalogue number 2018-01.

Occurrence

The new mineral sbacchiite was found in a fossil fumarole at the eastern rim of the crater in the so-called “cotunnite pit” (latitude 40° 49’ 21.98” N, longitude 14° 25’ 43.66” E), where other rare minerals were also discovered such as artroeite $\text{Pb}[\text{AlF}_3(\text{OH})_2]$ (Campostrini & Gramaccioli 2005), ammineite $[\text{CuCl}_2(\text{NH}_3)_2]$ (Russo & Campostrini, 2011), fluornatrocoulsellite $\text{CaNa}_3\text{AlMg}_3\text{F}_{14}$ (Russo *et al.* 2014), and parascandolaite KMgF_3 (Demartin *et al.* 2014). The formation of sbacchiite certainly took place between 1948-1960 or shortly thereafter (see below). It is not a real sublimate, but rather a high temperature encrustation, as HF attacked the rock extracting aluminum and calcium. The mineral is extremely rare and was found in one specimen only of approximate diameter 7 cm, that was trimmed into five smaller samples. It forms small aggregates of crystals up to about 60 μm in length, with a very steep bipyramidal habit, elongated along [100] and truncated by the (100) pinacoid (Figures 1-2). Associated minerals are gearsksutite, usovite, creedite and opal.

Physical and optical properties

Crystals of sbacchiite are transparent or translucent and colorless, with vitreous lustre and white streak. The tenacity is brittle. No distinct cleavage is observed. The mineral does not fluoresce in long- or short-wave ultraviolet light. No twinning is apparent. The density, measured by flotation in a diiodomethane/benzene solution is 3.08(2) g/cm^3 , that calculated using the empirical formula and unit-cell data is 3.116 g/cm^3 . Due to the minute size of the crystals the Mohs hardness could not be determined. Optically, sbacchiite is biaxial (+), with $\alpha = 1.379(4)$, $\beta = 1.384(4)$, $\gamma = 1.390(4)$ (measured in white light). The $2V$ measured on a spindle stage is $83(2)^\circ$; the calculated $2V$ is 85.1. The mean refractive index is 1.384, that predicted using the empirical electronic polarizabilities of ions (Shannon & Fisher, 2016), is 1.382.

Chemical Analysis

Quantitative chemical analyses (10) were carried out in EDS mode using a JEOL JSM 5500 LV scanning electron microscope equipped with an IXRF EDS 2000 microprobe (20 kV excitation voltage, 10 pA beam current, 2 μm beam diameter). This analytical method was chosen because crystal intergrowths did not take a good polish and was impossible to prepare a flat polished sample; moreover the crystals are severely damaged by using the WDS technique, even with a low voltage and current and a large diameter of the electron beam. In this case, as reported by Ruste (1979) and Acquafredda & Paglionico (2004), the EDS detector gives more accurate analyses of small volumes of investigated sample also with a probe current lower than 1 nA. This method gives good results also when collecting X-rays emitted from a non perfectly flat surface of the specimen. X-ray intensities were converted to wt% by ZAF quantitative analysis software. The standards employed were: fluorite for Ca and F and spinel for Al and Mg. Element concentrations were measured using the $K\alpha$ lines. The mean analytical results are reported in Table 1. No amounts of other elements above 0.1 wt% were detected. The empirical formula (based on 10 *apfu*) is: $(\text{Ca}_{2.02}\text{Mg}_{0.03})_{\Sigma 2.05} \text{Al}_{0.99}\text{F}_{6.97}$. The simplified formula is Ca_2AlF_7 , which requires 55.38 F, 11.24 Al and 33.38 Ca (wt%).

X-ray crystallography and crystal structure determination

The X-ray powder-diffraction pattern (Table 2), obtained using a conventional Bruker D8 diffractometer, with graphite monochromatized $\text{CuK}\alpha$ radiation, is in good agreement with that of the synthetic phase. The unit cell parameters refined from powder data using the UNITCELL software (Holland & Redfern, 1997) are $a = 7.674(1) \text{ \AA}$, $b = 6.996(1) \text{ \AA}$, $c = 9.553(1) \text{ \AA}$, $V = 512.9(1) \text{ \AA}^3$. From a needle-shaped crystal fragment (approximately $0.05 \times 0.01 \times 0.01 \text{ mm}$) 3655 diffracted intensities, corresponding to a complete scan of the reciprocal lattice up to $2\theta = 53.88^\circ$, were collected at room temperature using a Bruker Apex II diffractometer, equipped with a 2K CCD detector and $\text{MoK}\alpha$ radiation ($\lambda = 0.71073 \text{ \AA}$). A 90 seconds frame-time and a 0.5° frame width were used. The intensity data were reduced using the program *SAINT* (Bruker, 2001), and corrected for Lorentz,

polarization and background. An absorption correction ($\mu = 2.47 \text{ mm}^{-1}$, $T_{\min} = 0.735$) was applied using the *SADABS* program (Sheldrick, 2000). Starting from the atomic positions reported by Domsele & Hoppe (1980), the structure was refined anisotropically with the *SHELXL-2017* program (Sheldrick, 2015), implemented in the WinGX program (Farrugia, 1999). The refinement converged to a final $R = 0.0479$ for 457 observed reflections [$I > 2\sigma(I)$]. Details about the data collection and refinement are summarized in Table 3. Final atom coordinates and anisotropic displacement parameters are reported in Table 4. Selected interatomic distances are reported in Table 5.

Description of the crystal structure and discussion

Perspective views of the crystal structure of sbacchiite are reported in Figures 3 - 4. The asymmetric unit contains one Al^{3+} and two independent Ca^{2+} cations and five fluorine anions. Al is octahedrally coordinated by six fluorine atoms with Al-F distances in the range 1.768(4)-1.812(2) Å. The arrangement of F around Ca(1) (Figure 5) conforms to a distorted pentagonal bipyramid (C.N. 7; Ca-F distances in the range 2.224(4)-2.392(2) Å), similar to that observed in jakobssonite CaAlF_5 (Balić-Žunić *et al.* 2012) and that around Ca(2) to a very distorted polyhedron (C.N. 7+1 Ca-F distances in the range 2.262(4)-3.004(4) Å). All the fluorine atoms have C.N. 3, F(1), F(2) and F(3) are surrounded by three cations in a plane whereas, in case of F(4) and more pronounced for F(5), the anions are slightly out of plane. The bond-valence analysis (Table 6) confirms the crystal-chemical soundness of the crystal structure and the expected values for the valence of the Ca^{2+} , Al^{3+} and F^- ions. The whole structure framework is made up of linkages of “isolated” $[\text{AlF}_6]$ octahedra, $[\text{CaF}_7]$ and $[\text{CaF}_8]$ polyhedra. “Isolated” $[\text{AlF}_6]$ octahedra have also been observed in carlhintzeite $\text{Ca}_2\text{AlF}_7 \cdot \text{H}_2\text{O}$ (Kampf *et al.*, 2010), where two independent Al^{3+} cations are present but with a different environment. In carlhintzeite, one Al octahedron is face-sharing of two opposite faces with two Ca polyhedra and the other one is edge-sharing two opposite F-F edges: In sbacchiite, only one face is shared with the adjacent Ca(2) polyhedron and on the opposite side an edge and a corner of the same face are shared with two adjacent Ca(1) polyhedra (Figure 6). The structure of jakobssonite, CaAlF_5

contains instead vertex-sharing chains of $[\text{AlF}_6]$ octahedra, interconnected by chains of $[\text{CaF}_7]$ pentagonal bipyramids. In the other minerals with similar chemical constituents, whose structure is known *i.e.* gearsutite $\text{CaAlF}_4(\text{OH})\cdot\text{H}_2\text{O}$ (Marchetti & Perchiazzi, 2000) and prosopite $\text{CaAl}_2\text{F}_4(\text{OH})_4$ (Giacovazzo & Menchetti, 1969; Pudovnika *et al.* 1973), the Al octahedra are not isolated but arranged as edge-sharing dimers for the former or as edge-sharing chains for the latter.

In sbacchiite, the coordination polyhedra around Ca are linked by common edges in the sequence Ca(1)-Ca(2)-Ca(1)... along [010] and the same holds for the connection along [001]. Along [100] only the pentagonal bipyramids around Ca(1) are connected by bridging corners. In carlhintzeite all the Ca cations are instead 8-coordinated, and their linkage can be envisioned as a framework in which edge-sharing chains along [010] are cross-linked by edge sharing.

As already observed in carlhintzeite and gearsutite the distortion from the idealized geometry in the Ca polyhedra is clearly related to the way in which these polyhedra are linked. The lengths of their F...F edges can be correlated with their linkages to the $[\text{AlF}_6]$ octahedra and to the other Ca polyhedra, the shortest F...F edges corresponding to those shared with the $[\text{AlF}_6]$ octahedra. It is interesting to point out that in sbacchiite, prosopite, gearsutite and carlhintzeite the direction of the chains made by the Ca polyhedral determines a comparable unit-cell parameter. The chains in prosopite and gearsutite are parallel to the *c* cell parameter and correspond to cell parameters of 7.32 and 6.978(1) Å, respectively. In carlhintzeite the chain direction is parallel to the *b* unit cell parameter of 6.9670(5) Å, and for sbacchiite the corresponding value is 6.993(1) Å.

The discovery of sbacchiite in the fumaroles related to the 1944 eruption adds a new piece to the knowledge of the products formed when temperatures were higher than today, and confirms that fluorides deriving from reaction of HF with the surrounding rocks were the most common phases deposited. Formation of opal, which normally encrusts most of the occurring minerals and derives from leaching of the rock-forming silica and silicates, seems to be the last stage of a solid phase deposition. At present only water vapor is the main constituent of the fumarolic gases and formation of other mineral species is not observed.

Acknowledgements

Valuable suggestions and constructing comments for improving this paper have been given by A.R. Kampf and O. I. Siidra.

References

- Acquafredda, P. & Paglionico, A. (2004): SEM-EDS microanalyses of micro-phenocrysts of Mediterranean obsidians: a preliminary approach to source discrimination. *European Journal of Mineralogy*, **16**, 419–429.
- Balić-Žunić, T., Garavelli, A., Mitolo, D. Acquafredda, P., Leonardsen, E. (2012): Jakobssonite, CaAlF_5 , a new mineral from fumaroles at the Eldfell and Hekla volcanoes, Iceland. *Mineralogical Magazine*, **76**, 751–760.
- Brese, N.E. & O’Keeffe, M. (1991): Bond-valence parameters for solids. *Acta Crystallographica*, **B47**, 192–197.
- Brown, I.D. & Altermatt, D. (1985): Bond-valence parameters from a systematic analysis of the inorganic crystal structure database. *Acta Crystallographica*, **B41**, 244–247.
- Bruker (2001): SAINT, Bruker AXS Inc., Madison, Wisconsin.
- Campostrini, I. & Gramaccioli, C.M. (2005): Artroeite del Monte Somma-Vesuvio, secondo ritrovamento mondiale. *Rivista Mineralogica Italiana*, **29**, 1, 50–52.
- Demartin, F., Campostrini, I., Castellano, C., Russo, M. (2014): Parascandolaite, KMgF_3 , a new perovskite-type fluoride from Vesuvius, *Physics and Chemistry of Minerals*, **41**, 403–407.
- Domsele, R. & Hoppe, R., (1980): The crystal structure of Ca_2AlF_7 . *Zeitschrift für Kristallographie*, **153**, 317–328.
- Farrugia, L.J. (1999): WinGX suite for small-molecule single-crystal crystallography. *Journal of Applied Crystallography*, **32**, 837–838.
- Fischer, R.X. & Tillmanns, E. (1988): The equivalent isotropic displacement factor. *Acta Crystallographica*, **C44**, 775–776.

- 221 Giacobazzo, C. & Menchetti, S. (1969): The crystal structure of prosopite. *Naturwissenschaften*, **56**,
 222 86–87.
- 223 Holland, T.J.B. & Redfern, S.A.T. (1997): Unit cell refinement from powder diffraction data: the use
 224 of regression diagnostics. *Mineralogical Magazine*, **61**, 65–77.
- 225 Kampf, A.R., Colombo, F., Gonzalez del Tanago, J. (2010): Carlhintzeite, $\text{Ca}_2\text{AlF}_7 \cdot \text{H}_2\text{O}$ from the
 226 Gigante granitic pegmatite, Cordoba Province, Argentina: description and crystal structure.
 227 *Mineralogical Magazine*, **74**, 623–632.
- 228 Marchetti, F. & Perchiazzi, N. (2000): The crystal structure of gearksutite $\text{CaAlF}_4(\text{OH}) \cdot \text{H}_2\text{O}$.
 229 *American Mineralogist*, **85**, 231–235.
- 230 Parascandola, A. (1951): I minerali del Vesuvio nella eruzione del marzo 1944 e quelli formati
 231 durante l'attuale periodo di riposo. *Bollettino della Società Geologica Italiana*, **70**, 523–526.
- 232 _____ (1960): Notizie vesuviane. Il Vesuvio dal marzo 1948 al dicembre 1958. *Bollettino*
 233 *della Società dei Naturalisti in Napoli*, **68**, 184 pp., 4 figg., 20 tavv.
- 234 _____ (1961): Notizie vesuviane. Il Vesuvio dal gennaio 1959 al dicembre 1960. *Bollettino*
 235 *della Società dei Naturalisti in Napoli*, **69**, 263–298, 10 tavv.
- 236 Pudovkina, Z.V., Chernitsova, N.M., Pyatenko, Y.A. (1973): Refinement of the crystalline structure
 237 of prosopite $\text{CaAl}_2\text{F}_4(\text{OH})_4$. *Journal of Structural Chemistry*, **14**, 345–347.
- 238 Russo, M. & Campostrini, I. (2011): Ammineite, matlockite and post 1944 Eruption Fumarolic
 239 Minerals at Vesuvius. *Plinius*, **37**, 312–312.
- 240 _____, _____, Demartin, F. (2014): Fumarolic Minerals after the 1944 Vesuvius Eruption.
 241 *Plinius*, **40**, 306–306.
- 242 Ruste, J. (1979): X-ray spectrometry. In Maurice, F., Meny, L., and Tixier, R., Eds., Microanalysis
 243 and Scanning Electron Microscopy, Summer School St-Martin-d'Hères, France, September 11–16
 244 (1978), 215–267. Les Editions de Physique, Orsay.

245 Shannon, R.D. & Fischer, R.X. (2016): Empirical electronic polarizabilities of ions for the prediction
 246 and interpretation of refractive indices: oxides and oxysalts. *American Mineralogist*, 101, 2288 –
 247 2300

248 Sheldrick, G.M. (2000): *SADABS Area-Detector Absorption Correction Program*, Bruker AXS Inc.,
 249 Madison, WI, USA.

250 _____ (2015): Crystal structure refinement with SHELXL. *Acta Crystallographica*, **C71**, 3–
 251 8.

Table captions

253 Table 1. Analytical data (in wt%) for sbacchiite (average of 10 analyses)

254 Table 2. X-ray powder-diffraction data for sbacchiite and comparison with the synthetic analogue

255 Table 3. Single-crystal diffraction data and refinement parameters for sbacchiite

256 Table 4. Atomic coordinates and displacement parameters [U_{eq}/U^{ij} , Å²] for sbacchiite

257 Table 5. Selected interatomic distances (Å) and angles (deg.) in sbacchiite

258 Table 6. Bond-valence analysis for sbacchiite

Figure captions

261 Figure 1. Sbacchiite with gearksutite on volcanic breccia (base width 3 mm)

262 Figure 2. SEM-BSE image of sbacchiite crystals

263 Figure 3. View of the crystal structure of sbacchiite along [100]

264

265 Figure 4. View of the crystal structure of sbacchiite along. [010]

266 Figure 5. The coordination polyhedron of the Ca²⁺ cations

267 Figure 6. The environment of the Al site

268

269

270

271

272

Table 1. Analytical data (in wt%) for sbacchite (average of 10 analyses)

Constituent	Mean	Range	Stand. Dev.	Probe Standard
F	54.67	54.06-55.22	0.51	Fluorite
Al	10.97	10.78-11.14	0.10	Spinel
Ca	33.41	32.98-34.57	0.32	Fluorite
Mg	0.26	0.17-0.30	0.05	Spinel
Total	99.31			

273

274 The empirical formula (based on 10 *apfu*) is: $(\text{Ca}_{2.02}\text{Mg}_{0.03})_{\Sigma 2.05} \text{Al}_{0.99}\text{F}_{6.97}$

275 The simplified formula is Ca_2AlF_7 , which requires 55.38 F, 11.24 Al and 33.38 Ca (wt%)

276

277

278 Table 2. X-ray powder-diffraction data for sbacchiite and comparison with the synthetic analogue

279

Sbacchiite*		Sbacchiite**		Synthetic Ca ₂ AlF ₇ (Domsele & Hoppe, 1980)			
<i>d</i> (Å) (calc.)	<i>I</i> / <i>I</i> ₀ (calc.)	<i>d</i> (Å) (obs.)	<i>I</i> / <i>I</i> ₀ (obs.)	<i>d</i> (Å) (obs.)	<i>d</i> (Å) (calc.)	<i>I</i> / <i>I</i> ₀ (obs.)	<i>h k l</i>
5.982	5	5.986	6	5.9910	5.9871	7	1 0 1
4.546	3	4.550	2	4.5483	4.5493	3	1 1 1
3.833	38	3.840	45	3.8412	3.8426	40	2 0 0
3.558	72	3.563	85	3.5651	3.5648	90	2 0 1
3.497	100	3.499	100	3.4983	3.4989	100	0 2 0
3.361	3	3.366	5	3.3675	3.3682	3	2 1 0
3.171	10	3.174	15	3.1762	3.1764	13	2 1 1
3.018	1	3.020	2	3.0193	3.0209	3	1 2 1
2.991	8	2.990	10	2.9950	2.9935	13	2 0 2
2.944	4	2.941	3	2.9413	2.9408	3	1 0 3
2.901	46	2.899	55	2.8973	2.8974	53	0 1 3
2.823	1			2.8220	2.8223	3	0 2 2
2.750	22	2.750	30	2.7521	2.7523	33	2 1 2
2.713	8	2.710	10	2.7121	2.7111	13	1 1 3
2.649	2	2.647	5	2.6493	2.6493	7	1 2 2
2.494	2	2.495	4	2.4976	2.4971	7	2 2 1
2.468	2	2.470	5	2.4747	2.4742	7	3 0 1
2.451	6	2.449	8	2.4518	2.4513	10	2 0 3
2.391	1			2.3880	2.3873	3	0 0 4
2.328	1			2.3341	2.3327	3	3 1 1
2.313	4	2.314	5	2.3135	2.3135	7	2 1 3
2.283	17	2.281	20	2.2808	2.2798	30	1 0 4
2.263	5			2.2662	2.2660	3	0 3 1
2.253	61	2.255	52	2.2578	2.2573	50	3 0 2
2.172	23	2.173	36	2.1736	2.1735	43	1 3 1
2.029	8	2.028	10	2.0282	2.0278	13	2 0 4

280

281 * Pattern calculated on the basis of the single crystal data and structure refinement

282 ** Experimental pattern obtained using a Bruker D8 diffractometer (Cu K α radiation)

283

284

Table 3. Single-crystal diffraction data and refinement parameters for sbacchiite

Crystal system	orthorhombic
Space Group	<i>Pnma</i> (no. 62)
<i>a</i> (Å)	7.665(2)
<i>b</i> (Å)	6.993(1)
<i>c</i> (Å)	9.566(2)
<i>V</i> (Å ³)	512.2(2)
<i>Z</i>	4
Radiation	MoK α
μ (mm ⁻¹)	2.47
D _{calc} (g cm ⁻³)	3.111
Reflections measured	3655
Independent reflections	590
Observed reflections [<i>I</i> > 2 σ (<i>I</i>)]	457
Parameters refined	55
Final <i>R</i> [<i>I</i> > 2 σ (<i>I</i>)] and <i>wR</i> 2 (all data)	0.0479, 0.0863
Goof	1.157

Notes: $R = \sum ||F_o| - |F_c|| / \sum |F_o|$; $wR2 = \{ \sum [w(F_o^2 - F_c^2)^2] / \sum [w(F_o^2)^2] \}^{1/2}$;

$w = 1 / [\sigma^2(F_o^2) + (0.0328q)^2 + 0.8790q]$ where $q = [\max(0, F_o^2) + 2F_c^2] / 3$;

Goof = $\{ \sum [w(F_o^2 - F_c^2)] / (n-p) \}^{1/2}$ where *n* is the number of reflections and *p* is the number of refined parameters.

Table 4. Atomic coordinates and displacement parameters [U_{eq}/U^{ij} , Å²] for sbacchiite

Atom	Wyckoff letter	x/a	y/b	z/c	U_{eq}
Al	4c	0.3088(2)	1/4	0.05621(17)	0.0075(4)
Ca1	4c	0.11312(17)	1/4	0.74096(12)	0.0120(3)
Ca2	4c	0.80132(16)	1/4	0.10650(12)	0.0107(3)
F1	4c	0.3717(5)	1/4	0.6299(3)	0.0176(8)
F2	4c	0.0297(4)	1/4	0.5084(4)	0.0142(8)
F3	4c	0.0954(5)	1/4	0.1263(4)	0.0258(10)
F4	8d	0.2486(3)	0.07395(3)	0.92591(2)	0.0158(6)
F5	8d	0.3683(4)	0.0716(3)	0.1842(2)	0.0153(6)

Atom	U^{11}	U^{22}	U^{33}	U^{23}	U^{13}	U^{12}
Al	0.0092(9)	0.0059(8)	0.0074(9)	0	0.0004(7)	0
Ca1	0.0128(7)	0.0109(6)	0.0122(6)	0	0.0014(5)	0
Ca2	0.0132(7)	0.0073(6)	0.0116(6)	0	-0.0033(5)	0
F1	0.017(2)	0.019(2)	0.016(2)	0	-0.004(2)	0
F2	0.008(2)	0.018(2)	0.018(2)	0	-0.005(2)	0
F3	0.011(2)	0.030(2)	0.036(2)	0	0.011(2)	0
F4	0.022(2)	0.008(1)	0.017(1)	-0.001(1)	-0.010(1)	-0.001(1)
F5	0.026(2)	0.008(1)	0.012(1)	0.002(1)	-0.002(1)	0.001(1)

The anisotropic displacement factor exponent takes the form:

$$-2\pi^2(U^{11}h^2(a^*)^2 + \dots + 2U^{12}hka^*b^* + \dots); U_{eq} \text{ according to Fischer and Tillmanns (1988).}$$

Table 5. Selected interatomic distances (Å) and angles (deg.) in sbacchiite

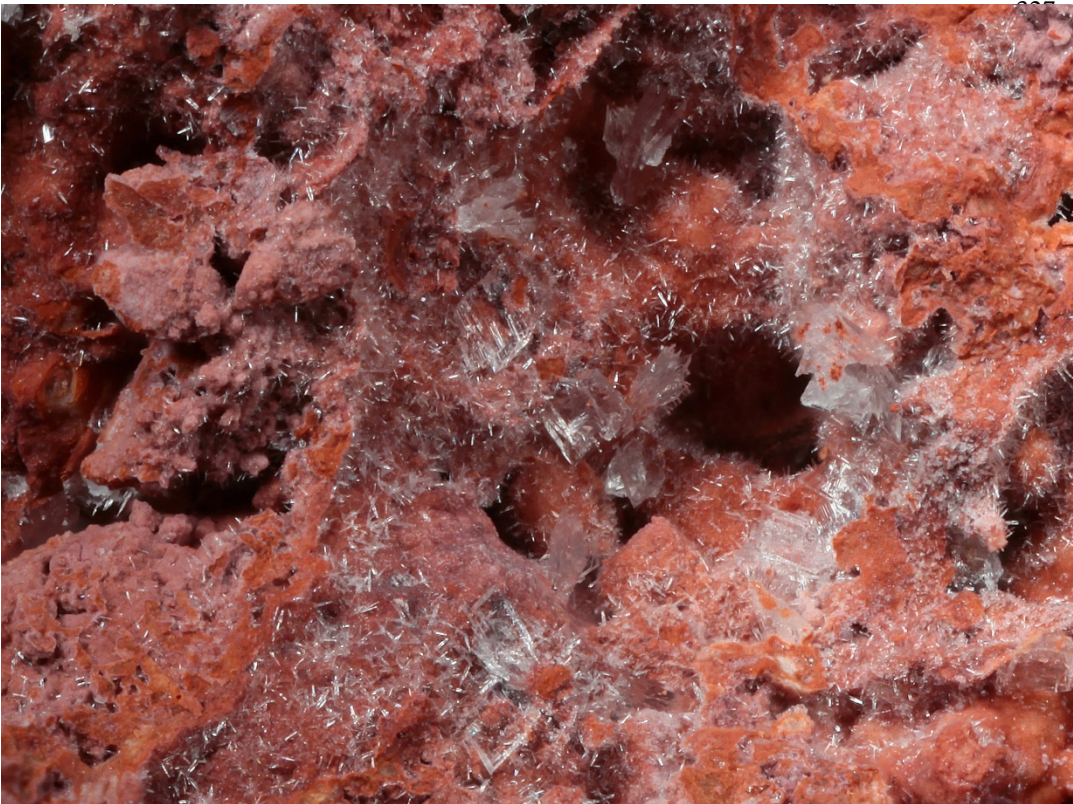
Al-F2	1.802(4)	Al-F4 (×2)	1.812(2)
Al-F3	1.768(4)	Al-F5 (×2)	1.806(2)
<Al-F>	1.801		
Ca1-F1	2.224(4)	Ca2-F1	2.325(3)
Ca1-F1	2.249(4)	Ca2-F2	2.354(4)
Ca1-F2	2.315(4)	Ca2-F3	2.262(4)
Ca1-F4 (×2)	2.392(2)	Ca2-F3	3.004(4)
Ca1-F5 (×2)	2.318(2)	Ca2-F4 (×2)	2.318(2)
<Ca1-F>	2.315	Ca2-F5 (×2)	2.414(2)
		<Ca2-F>	2.426

Table 6. Bond-valence analysis for sbacchiite.

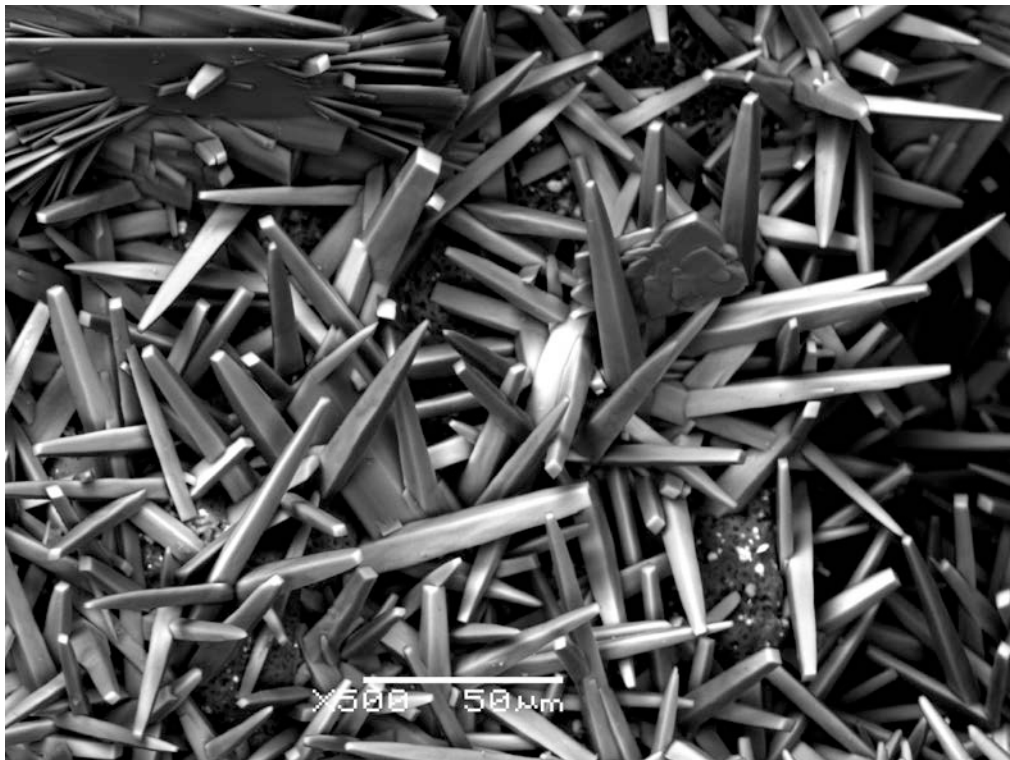
	F1	F2	F3	F4	F5	Σc
Al		0.499	0.547	0.485×2→ 0.485↓	0.491×2→ 0.491↓	2.998
Ca1	0.355→ 0.333↓	0.279		0.226×2→ 0.226↓	0.276×2→ 0.276↓	1.971
Ca2	0.272	0.247	0.323→ 0.043↓	0.278×2→ 0.278↓	0.215×2→ 0.215↓	1.871
Σa	0.960	1.025	0.913	0.989	0.982	

Bond-valence parameters from Brown & Altermatt (1985), Brese & O'Keeffe (1991). Values are expressed in valence units (vu).

325 Figure 1. Sbacchiite with gearsutite on volcanic breccia (base width 3 mm)
326



340
341 Figure 2. SEM-BSE image of sbacchiite crystals



342

Figure 3. View of the crystal structure of sbacchiite along [100]

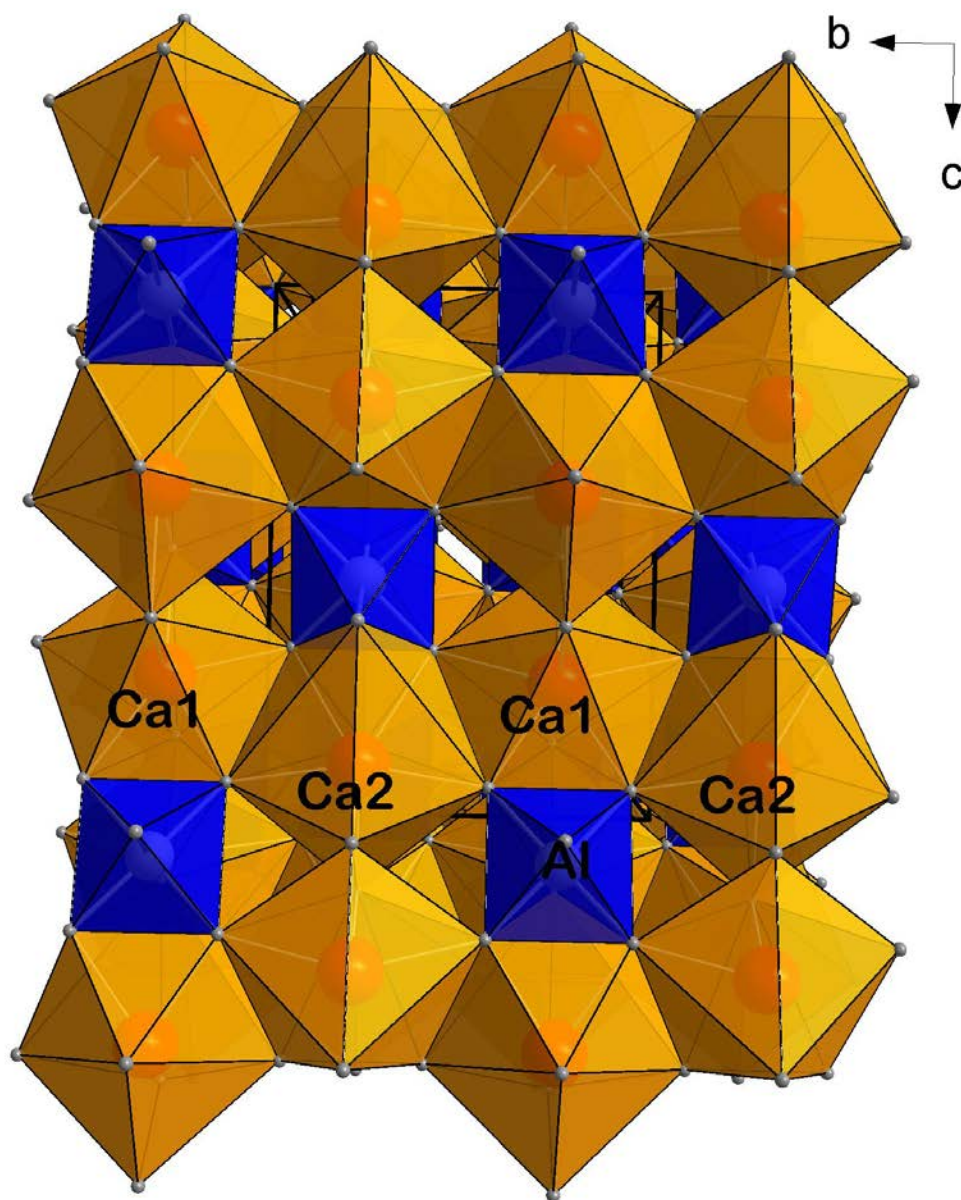
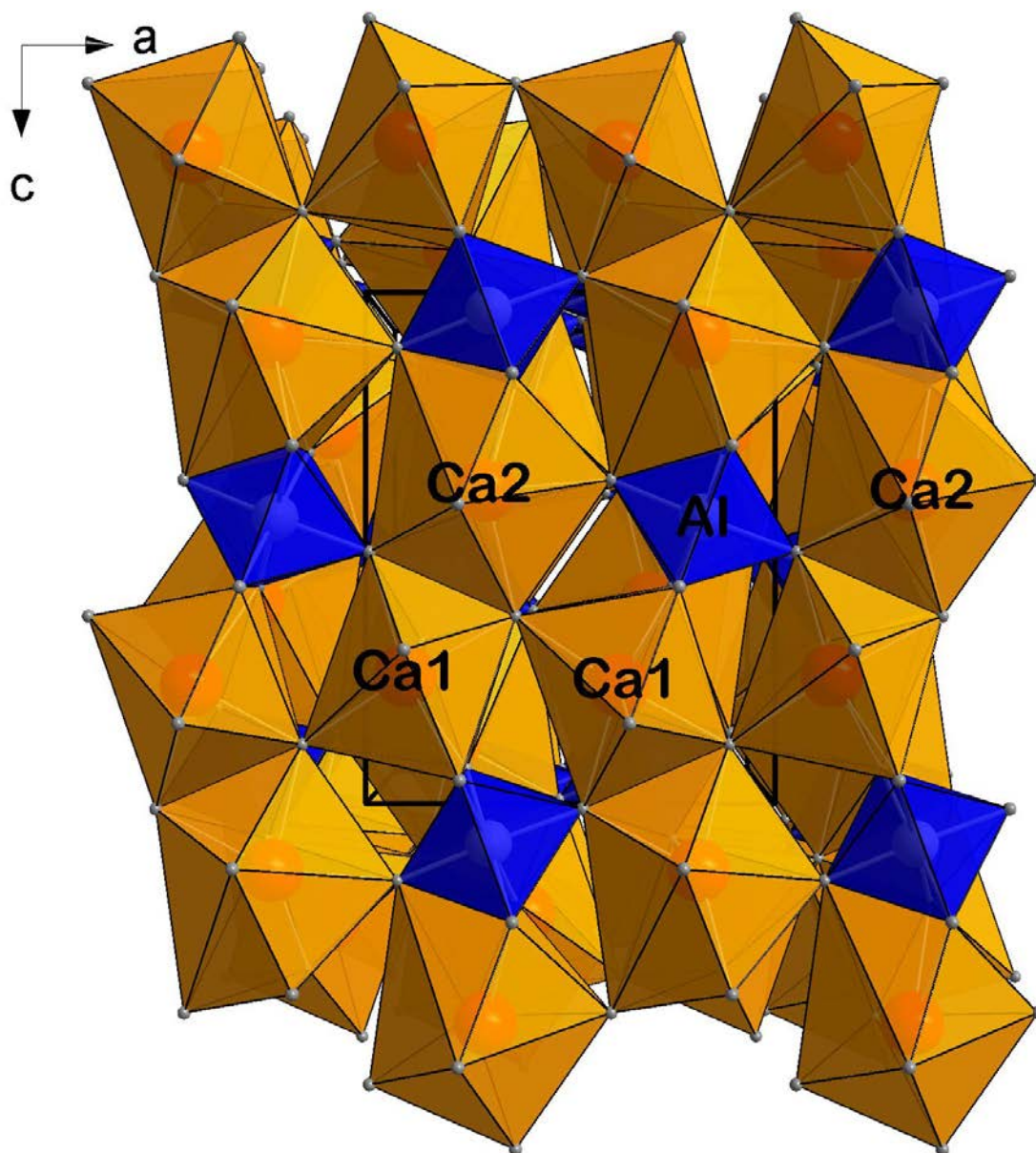


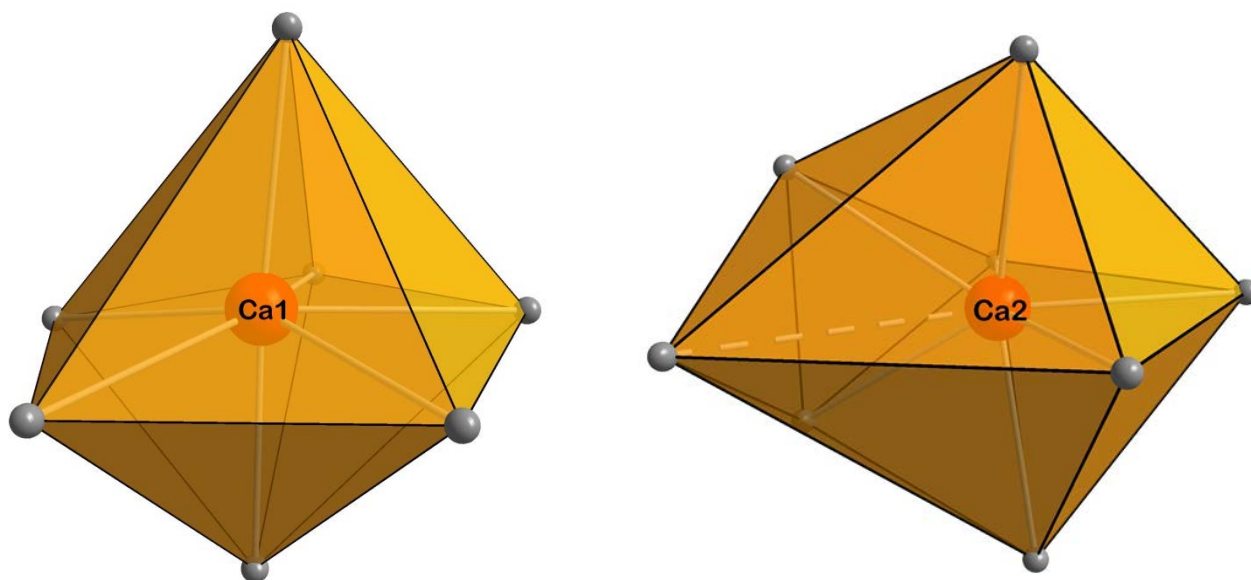
Figure 4. View of the crystal structure of sbacchiite along [010]



354

355 Figure 5. The coordination polyhedron of the Ca^{2+} cations

356



360

361

362 Figure 6. The environment of the Al site

363

